

## Alignment in Molecular Excitation for 3.22-keV $H_2^+$ -He Collisions

D. H. Jaecks, O. Yenen, M. Natarajan, and D. Mueller<sup>(a)</sup>

*Behlen Laboratory of Physics, University of Nebraska, Lincoln, Nebraska 68588*

(Received 27 December 1982)

Electronic alignment in molecular excitation, relative to a specific internuclear axis orientation, has been observed for the first time, enabling specific detailed checks of the quasidiatomic molecular-orbital model in kiloelectronvolt atom-molecule collisions. The alignment was determined from the polarization of  $L_\alpha$  radiation, resulting from the collision process  $H_2^+ + He \rightarrow H_2^{+*} + He \rightarrow H^+ + H(2p) + He$ , for specific laboratory scattering angles of  $H^+$ . The results suggest that, as in many ion-atom systems, rotational coupling is the dominant excitation mechanism.

PACS numbers: 34.50.Ez

Since the early experimental work of Ziemba *et al.*,<sup>1</sup> and the subsequent theoretical framework of Fano and Lichten,<sup>2</sup> great strides have been made in our understanding of a range of atomic collision processes. Recent work of Doweck *et al.*,<sup>3</sup> has successfully extended some of the basic ideas that have proven so valuable in describing binary systems to triatomic systems, that is, to ion/atom-molecule collisions. Specifically, they have been able to provide insights into the inelastic processes of He- and He<sup>+</sup>-H<sub>2</sub>(D<sub>2</sub>) collisions, by incorporating a quasidiatomic molecular-orbital (MO) correlation diagram to describe the collision, although the system is a triatomic one. In addition, they have presented three-dimensional correlation surfaces for the He-H<sub>2</sub> system. The quasidiatomic MO correlation diagram used by Doweck *et al.* is shown in Fig. 1. In this figure the H<sub>2</sub>-He MO diagram is constructed in analogy to H-He; one expects that this should give a reason-

able picture of the possible electron promotion mechanisms, when the H<sub>2</sub><sup>+</sup> internuclear separation is smaller than the distance between He and H<sub>2</sub><sup>+</sup> centers of mass. Clearly, our understanding of inelastic processes will be greatly advanced if the limits of this generalization of the diatomic to the triatomic can be established.

We wish to report new measurements that indicate the general efficacy of this MO correlation picture and point out how it can be used to understand a range of inelastic processes in H<sub>2</sub><sup>+</sup> + He collisions.

The specific experiment that we have performed is the measurement of the polarization of  $L_\alpha$  radiation in coincidence with the scattered proton that results from the process  $H_2^+ + He \rightarrow H_2^{+*} + He \rightarrow H^+ + H(2p) + He$ . For distant collisions that result in negligible deflection of the H<sub>2</sub><sup>+</sup> c.m., the direction of the H<sup>+</sup> provides information about the final orientation of the H<sub>2</sub><sup>+</sup> internuclear axis and the c.m. H<sup>+</sup> velocity, while the  $L_\alpha$  polarization provides information about the alignment of H(2p) relative to that axis.

Details of the apparatus have been discussed elsewhere.<sup>4</sup> The essential features of the apparatus are a needle gas jet to provide a target, a solar-blind  $L_\alpha$  detector, and a LiF Brewster-angle polarizer. The  $L_\alpha$  photons are detected in a direction perpendicular to a plane defined by the momenta of the incident H<sub>2</sub><sup>+</sup> beam and the scattered H<sup>+</sup> as indicated in Fig. 2.

The measured  $L_\alpha$  intensities  $I(\beta)$ , for specific polarization angles  $\beta$  at specific H<sup>+</sup> scattering angles, as determined by coincidence measurements, are shown in Fig. 3 along with the least-squares fit to the data of a general dipole intensity pattern. The measurements indicate that as the scattering angle is increased, the polarization distribution becomes increasingly "pinched" until at  $\theta = \pm 3.25$ , the ratio of  $I_{max}/I_{min}$  is the maximum allowed by the atomic precession due

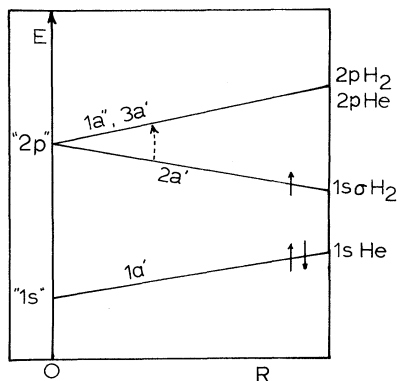


FIG. 1. Quasidiatomic MO diagram for the He-H<sub>2</sub> system. The two arrows on curve 1a' refer to the two electrons of He and the one on curve 2a' shows the only electron of H<sub>2</sub><sup>+</sup>. The 2p He and 2p H<sub>2</sub> states, being nearly degenerate, are not shown separately. The experimental results suggest that 1sσ H<sub>2</sub><sup>+</sup> (curve 2a') is promoted to 2pπ H<sub>2</sub><sup>+</sup> (curve 3a') by rotational coupling.

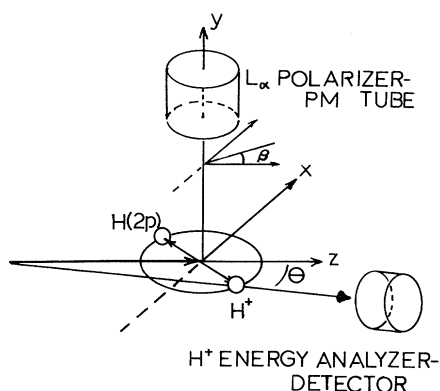


FIG. 2. Schematic arrangement for  $H^+ - L_\alpha$  coincidence measurement.

to spin-orbit coupling.<sup>5</sup>

Also schematically shown in Fig. 3 is the range of  $H_2^+$  internuclear-axis orientations at angles  $\alpha$  relative to the beam direction that contribute to the  $H^+ - L_\alpha$  coincidence signal. The energy analyzer does not have sufficient resolution to distinguish different  $H^+$  laboratory velocity vectors

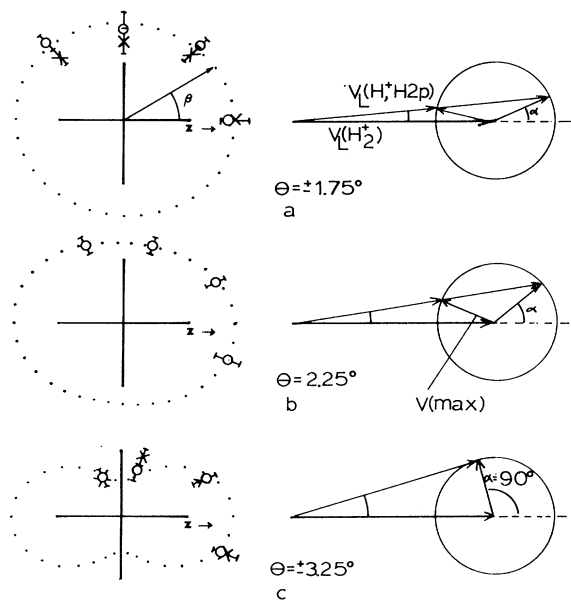


FIG. 3. Left-hand side: Polarization measurements  $I(\beta)$  at different  $H^+$  scattering angles for 3.22-keV  $H_2^+ - He$  collisions. The beam direction is shown by  $z$ . Right-hand side: Velocity diagrams showing the variation in range of  $H_2^+$  axis orientations which give rise to the observed polarization patterns as a function of  $H^+$  laboratory scattering angle. The speed of the dissociation products being much smaller than that of the center of mass, the radii of the circles are greatly exaggerated and  $\alpha = 90^\circ$  is schematically shown.

that result from various c.m.  $H^+$  velocities and ( $H_2^{+*}$ ) orientations. The c.m. velocity circle exaggerated in Fig. 3 and given by  $v(\max)$  represents the maximum velocity of  $H^+$  in the  $H_2^+$  c.m. frame. This velocity corresponds to a c.m. energy of about 5 eV above the  $H^+ + H(2p)$  dissociation limit and results from a vertical Franck-Condon transition to the  $2p\pi_u$  state at an internuclear separation of  $1.5a_0$  as indicated in Fig. 4. We have chosen  $1.5a_0$  because this value corresponds to the classical turning point of the  $\nu = 3$  vibrational state, the state with maximum population probability as determined by the Franck-Condon principle in  $H_2^+$  formation from  $H_2$ .<sup>6</sup> From Fig. 3(c), we see that a 5-eV c.m.  $H^+$  energy corresponds to a maximum laboratory scattering angle of  $3.2^\circ$ , with the  $H_2^+$  internuclear axis perpendicular to the initial ion beam direction. It is at this angle (internuclear orientation) we ob-

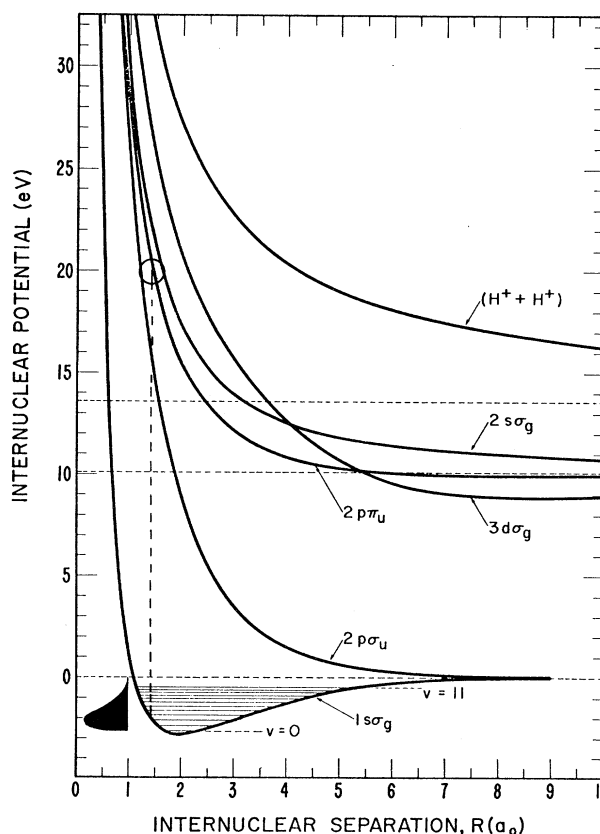


FIG. 4. Relevant  $H_2^+$  potential curves. For collisions in which the  $H_2^+$  internuclear-axis orientation is perpendicular to the beam direction, the  $H_2^+$  molecular ion is excited by a Franck-Condon type transition to the  $2p\pi_u$  state at an internuclear separation of 1.5 a.u. The maximum alignment of the  $H(2p)$  results from the subsequent dissociation of  $H_2^+(2p\pi_u)$ .

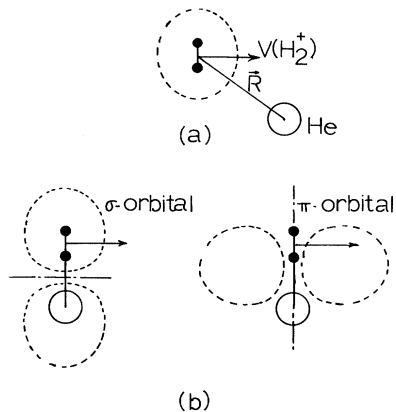


FIG. 5. (a)  $1s\sigma_g$  state of the incoming  $H_2^+$ . (b) Near distance of closest approach, the nodal planes of  $\sigma$ -like (parallel to the beam direction) and  $\pi$ -like (perpendicular to the beam direction) orbitals.

serve maximum alignment of the  $H(2p)$  resulting from the dissociation of  $(H_2^+)^*$ .

With the aid of the quasidiatomic MO correlation diagram and the polarization intensity measurements  $I(\beta)$ , we can obtain insights into the excitation mechanisms in  $H_2^+$ -He collisions. The polarization pattern  $I(\beta)$  for small  $H^+$  scattering angles,  $\theta$ , represents intensity contributions from a sum of  $H_2^+$  internuclear orientations and various c.m.  $H^+$  velocities as illustrated in Fig. 3. By  $\theta = \pm 3.25^\circ$ , only a small range of internuclear orientations and c.m.  $H^+$  velocities contribute to the observed  $L_\alpha$ - $H^+$  coincidence signal. Also at this angle we are observing  $H(2p) + H^+$  from dissociating states of  $H_2^{+*}$  that are excited near the highest possible point of the repulsive potential curves.

Focusing our attention on the results at this angle, we note that the polarization intensity of the  $L_\alpha$  radiation is that characteristic of  $2p_{\pm 1} \rightarrow 1s$  transitions, using the  $H_2^+$  internuclear axis as the quantization axis.<sup>5</sup> Thus, the observed final  $H(2p_{\pm 1}) + H^+$  state results from the excitation and decay of the  $\Pi_u$  state of  $H_2^+$ , a result consistent with using 5 eV as the c.m. energy of  $H^+$ .

These results can be interpreted within the context of the quasidiatomic description of the excitation mechanism for  $H_2^+$ -He collisions. Figure 5 diagrammatically illustrates the prediction of the MO diagram of Fig. 1, for the case of  $H^+$  scattering at  $3.25^\circ$  (internuclear axis perpendicular to the beam axis). Rotational coupling, that is,  $\sigma \rightarrow \pi$  transitions at the closest He- $H_2^+$  centers-of-mass distance, produces an excited  $\pi$ -like orbital

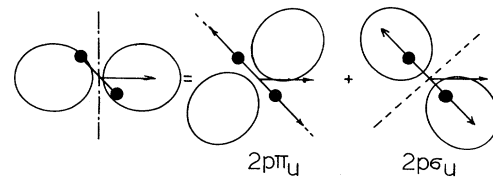


FIG. 6.  $2p\pi_u$  and  $2p\sigma_u$  wave functions for arbitrary internuclear orientation.

of the He- $H_2^+$  system, having for this orientation a nodal plane perpendicular to the beam axis. The wave function for the  $H_2^+$ -He system consists of a linear combination of the two wave functions having nodal character similar to that shown in Fig. 5. The excited-state wave function carried off by the  $H_2^+$  is then  $\pi$ -like in character, with the  $H_2^+$  internuclear axis in the nodal plane. Thus the final excited  $H_2^+$  orbital has ungerade symmetry.

As the excited  $H_2^+$  recedes from the He target the wave function remains frozen or locked into the  $H_2^+$  internuclear axis producing a large amplitude for exciting the  $\Pi_u$  state. Being a  $\Pi_u$  state, the system dissociates to  $H^+ + H(2p_{\pm 1})$  relative to the internuclear axis, that is, perpendicular to the beam direction, and provides the measured polarization distribution.

As shown in Fig. 6, other orientations  $\alpha$  lead to excitation of other states, since the space-fixed  $\Pi$ -like wave function can be written as a coherent linear combination of body-fixed  $\Pi$  and  $\sigma$  wave functions.

Thus the two dominant excitation channels should be to the  $2p\pi_u$  and  $2p\sigma_u$  states. At an  $H_2^+$  orientation perpendicular to the beam direction the excitation should be to the  $2p\pi_u$  state, while for a parallel orientation the  $2p\sigma_u$  state should dominate.

Thus the collision model here addresses a rather long outstanding problem in the understanding of molecular collision excitation and decay processes.<sup>7</sup> The problem was one of trying to interpret and reconcile the proton production in detailed Astron-band measurements with the fact that cross sections for  $L_\alpha$  production in  $H_2^+$ -He collisions<sup>7-10</sup> are of the same order of magnitude. The results here clearly suggest that both states play a role and the excitation should be of comparable magnitude.

This work was supported by the National Science Foundation.

(a) Present address: Joint Institute for Laboratory

Astrophysics, Boulder, Colo. 80302.

<sup>1</sup>E. P. Ziemba, G. J. Lockwood, G. H. Morgan, and E. Everhart, *Phys. Rev.* **118**, 1552 (1962).

<sup>2</sup>U. Fano and W. Lichten, *Phys. Rev. Lett.* **23**, 157 (1969).

<sup>3</sup>D. Doweck, D. Dhuicq, V. Sidis, and M. Barat, *Phys. Rev. A* **26**, 746 (1982).

<sup>4</sup>R. H. McKnight and D. H. Jaecks, *Phys. Rev. A* **4**, 2281 (1971).

<sup>5</sup>J. Macek and D. H. Jaecks, *Phys. Rev. A* **4**, 2288 (1971).

<sup>6</sup>Gordon H. Dunn and Bert Van Zyl, *Phys. Rev.* **154**,

40 (1967); Marcella M. Madsen and James Peek, *At. Data* **2**, 171 (1971).

<sup>7</sup>D. K. Gibson and J. Los, *Physica (Utrecht)* **35**, 258 (1967).

<sup>8</sup>Gordon H. Dunn, Ronald Geballe, and Donovan Pretzer, *Phys. Rev.* **128**, 2200 (1962).

<sup>9</sup>B. van Zyl, D. Jaecks, D. Pretzer, and R. Geballe, *Phys. Rev.* **136A**, 1561 (1964).

<sup>10</sup>D. Jaecks and E. Tynar, in *Proceedings of the Fourth International Conference on the Physics of Electronic and Atomic Collisions, Quebec, 1965* (Science Bookcrafters, Hastings-on-Hudson, 1965), p. 315.

## Precise Measurements of Hyperfine Structure in the $2^3P$ State of $^3\text{He}$

J. D. Prestage and E. A. Hinds

*Physics Department, Yale University, New Haven, Connecticut 06520*

and

F. M. J. Pichanick

*Department of Physics and Astronomy, University of Massachusetts, Amherst, Massachusetts 01003*

(Received 17 November 1982)

Transitions within the  $2^3P$  state of  $^3\text{He}$  were measured to determine the parameters  $C$ ,  $D$ , and  $E$  which represent respectively the contact, dipole, and tensor terms in the hyperfine Hamiltonian. For the first time, the effect of core polarization on the hyperfine structure has been detected. The present results are  $C = -4283.84(1)$  MHz,  $D = -28.02(6)$  MHz, and  $E = +7.08(2)$  MHz and are consistent with the theoretical values after the combined fine and hyperfine interactions with the  $2^1P$  state are taken into account in the analysis of the data.

PACS numbers: 35.10.Fk, 32.30.Bv

The spectra of excited states ( $1snl$ ) of  $^3\text{He}$  have been the subject of several recent experimental investigations. The techniques employed are level crossings and anticrossings,<sup>1</sup> various forms of Doppler-free laser spectroscopy,<sup>2,3</sup> and quantum beats in beam-foil spectra.<sup>4</sup> States of  $^3\text{He}$  which have been studied include  $n^3S$ ,  $n^3D$ , and  $n^1D$  up to  $n=6$ , and  $n^3P$  up to  $n=8$ . The measured intervals within these states are now known with accuracies ranging from 0.1 to 20 MHz. As the principal quantum number  $n$  increases, the  $^3\text{He}^+$  core dominates first the fine structure, then the exchange interaction, and ultimately (above  $n \sim 100$ ) the

gross level structure, leading to two ionization limits. We hope to explore these effects to a precision of about 0.03 MHz using an extension of the optical microwave technique reported here.

In this Letter we report a measurement of the  $1s2p^3P$  hyperfine structure which is 2 to 3 orders of magnitude more precise than earlier data. In particular we have measured with high precision the contribution of the  $p$  electron to the hyperfine structure, a phenomenon which was previously barely resolved from the noise,<sup>3</sup> and we have measured previously undetected core-polarization effects.

The hyperfine Hamiltonian is given by<sup>5</sup>

$$\mathcal{H}_{\text{hfs}} = -2\mu_0 \sum_{i=1}^2 \left\{ -\frac{8\pi}{3} (\vec{s}_i \cdot \vec{\mu}) \delta(\vec{r}_i) - \frac{1}{r_i^3} \vec{l}_i \cdot \vec{\mu} + \frac{1}{r_i^3} \left[ \vec{s}_i \cdot \vec{\mu} - \frac{3(\vec{s}_i \cdot \vec{r}_i)(\vec{\mu} \cdot \vec{r}_i)}{r_i^2} \right] \right\}. \quad (1)$$

The sum is taken over the two electrons,  $\vec{\mu}$  is the nuclear magnetic moment, and  $\vec{s}_i$ ,  $\vec{l}_i$ , and  $\vec{r}_i$  have the usual meanings for an individual electron.

Within a pure  $^3P$  state, Eq. (1) may be written

$$\mathcal{H}_{\text{hfs}} = C \vec{I} \cdot \vec{S} + D \vec{I} \cdot \vec{L} + (2\sqrt{10})E \vec{I} \cdot (\vec{S}C^{(2)})^1, \quad (2)$$